MEASURING THE EFFICIENCY OF THE TEXAS A&M POSITRON EMISSION TOMOGRAPH

A Thesis

by

WESLEY BLAKE LOEWER

Submitted to the Graduate College of
Texas A&M University
in partial fulfillment of the requirements for the degree of

MASTER OF SCIENCE

May 1988

Major Subject: Physics

MEASURING THE EFFICIENCY OF THE TEXAS A&M
POSITRON EMISSION TOMOGRAPH

A Thesis

by

WESLEY BLAKE LOEWER

Approved as to style and content by:

John A. McIntyre
(Chairman of Committee)

Thomas Meyer
(Member)

Rand Watson
(Member)

Richard Arnowitt
(Head of Department)

May 1988

ABSTRACT

Measuring the Efficiency of the Texas A&M
Positron Emission Tomograph. (May 1988)
Wesley Blake Loewer, B.S., Wheaton College
Chairman of Advisory Committee: Dr. John A. McIntyre

The Texas A&M University Positron Emission Tomograph (TAMU PET) detects the gamma rays which are emitted in positron-electron annihilation by using plastic scintillators and optical fibers to code the light given off by the scintillators. Such coding greatly reduces the number of photomultipliers necessary to detect scintillations, thus allowing improvement in resolution without being inhibited by cost. Light from a scintillation travels by means of total internal reflection along a row of an array of scintillators, through optical fibers to four photomultiplier tubes where the light from the scintillation is detected. All four photomultipliers must coincidentally detect the flash of light from the scintillator to determine the location of a gamma ray interaction. The efficiency at which a PET detects scintillations, in part, determines the clarity of the images produced.

This detection efficiency was measured for the TAMU PET by determining the number of scintillations occuring in a given scintillator and comparing that number to the number of scintillations from this scintillator actually detected by the fiber system of the TAMU PET. This detection efficiency was found to be 0.29 ± 0.015.

ACKNOWLEDGEMENTS

I would first of all like to thank my chairman, Dr. McIntyre, for his patience and persistence. Without his direction and guidence, none of this would have been possible. I would also like to thank Ruth Seidel and Lisa Dixon for their help and support all along the way. A special word of thanks also goes to Patricia McGough for doing all the dirty work and for being a regular person among a group of graduate students.

To my wife Jane,

who provided constant encouragement and friendship and

who was always there throughout the whole process.

TABLE OF CONTENTS

TABLE OF CONTENTS (continued)

LIST OF FIGURES

CHAPTER I

INTRODUCTION

The Texas A&M positron emission tomograph (TAMU PET) is an imaging device to be used in medical applications. As with all PET's, the subject is injected with a low level, positron emitting isotope. The positrons being emitted interact with nearby electrons, resulting in positron-electron annihilation. Products of this interaction include two gamma rays which are emitted nearly anti-parallel to each other. These two gamma rays are then detected by the PET. One of the important specifications of a PET is the effeciency at which it detects gamma rays. It is the goal of this research to measure this effeciency.

Previous PET's typically have used scintillators such as BGO or NaI(Tl) surrounding the patient to detect the gamma rays being emitted. Each scintillator would then be coupled to a photomultiplier tube to detect the light scintillations. The electric pulses coming from the photomultiplier tube could then be put through coincidence circuits so that pulses would only be recorded if both gamma rays were detected. This information could then be fed into a computer. Knowing the position of the two scintillators which detected the gamma rays allows the computer to reconstruct the path along which the gamma rays traveled from the positron-electron interaction. Given a large number of positron-electron interactions taking place, a computer can then pinpoint areas of the body which are giving off larger or smaller amounts of gamma ray radiation. This information can then be presented in a visual image for subsequent study.

PET's which use single scintillators coupled to single photomultiplier tubes are mechanically limited as to the resolution of the images they can produce. The

---

Journal model is *IEEE Transactions on Medical Imaging*.

resolution of a PET is roughly equal to half the spacing of the scintillators used. If each scintillator has a photomultiplier tube attached, it is easy to see that there is a limit as to the number of photomultiplier tubes that can be packed together in a ring. Also, the problem of cost becomes a factor when trying to improve the resolution. If the resolution were to be improved by a factor of two, then twice as many photomultiplier tubes would be needed.

The TAMU PET, however, uses a different approach in detecting the gamma rays. Plastic scintillators are used to surround the subject (Fig. 1). (The plastic scintillator used was NE102 made by Nuclear Enterprises. The same material is also made by Bicron under the name BC400.) Because gamma rays have a longer mean free path in plastic scintillator material than they do in BGO or NaI(Tl), several layers of plastic scintillators are used in each ring to stop more gamma rays. A number of these rings are placed side by side in order to cover a larger volume of the body. The TAMU PET does not have a photomultiplier tube connected to each scintillator but uses optical fibers to encode and transmit the light from the scintillators to the photomultiplier tubes. As a result, the spacing between plastic scintillators is limited only by the diameter of an optical fiber and therefore can be made very small. The TAMU PET design calls for rings consisting of 1024 scintillator wedges packed into each ring with 16 layers of scintillators in each wedge for a total of 16,384 scintillators per ring. Each scintillator is 1.0 cm in the radial direction and averages 2.4 mm in the azimuthal direction. If 8 rings are used, it brings the total number of scintillators used to 131,072. It is obvious that the large number of scintillators being used demands that a different coupling technique be incorporated than the one scintillator to one photomultiplier tube method.

Each scintillator surface is optically polished and is separated from its neighbor by a very thin layer of epoxy which has a slightly lower index of refraction than the

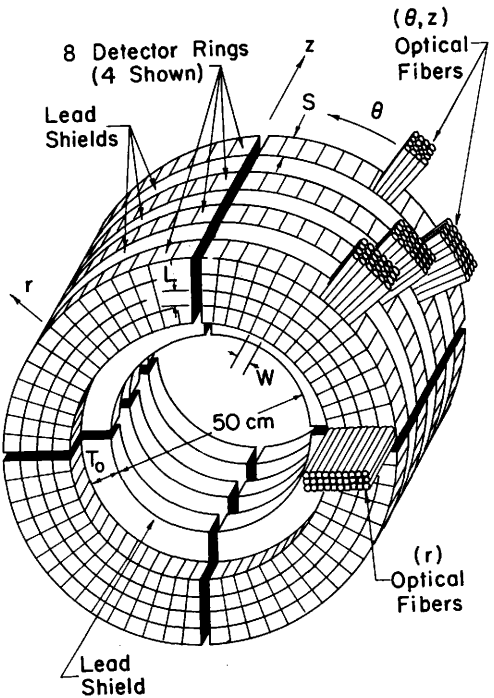

Fig. 1. Schematic of TAMU PET.

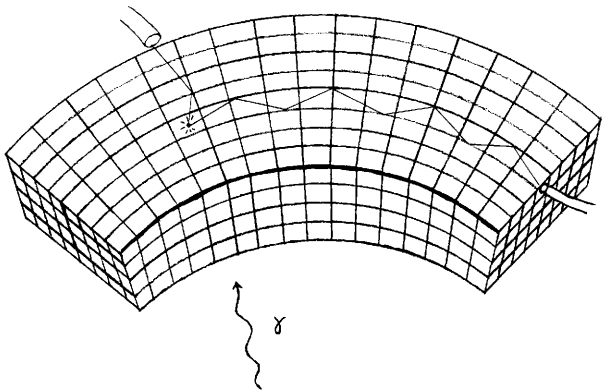

Fig. 2. Total internal reflection down rows of scintillators.

scintillator. When a scintillation occurs, light travels by means of internal reflection along the row and column of the array of polished scintillators (Fig. 2). The light is then collected by optical fibers and carried to photomultiplier tubes. The fibers are connected in such a way that each quarter ring is operated independently of the other three quarters. Each scintillator in a particular quarter ring is optically coupled by means of the optical fibers to one of two possible photomultiplier tubes. Each scintillator in a $\frac{1}{16}$th section of all the quarter rings is coupled to a single photomultiplier tube. Each scintillator in a particular column of every $\frac{1}{16}$th section is coupled to a single photomultiplier tube. Finally, each scintillator in a row is

coupled to one of two possible photomultiplier tubes. Therefore, the total number of photomultiplier tubes needed for an eight ring tomograph is (2 × 8 rings + 16 sections per quarter ring + 16 columns per section + 2 × 16 rows) × 4 quarter rings = 320 photomultiplier tubes to address (8 rings × 16 sections per quarter ring × 16 columns per section × 16 rows) × 4 quarter rings = 131072 scintillators.

Using the optical fiber coupling allows for large gains in improving resolution without being inhibited by cost. This design, however, is not without its drawbacks. One of the main difficulties is getting the light from the scintillator to the photomultiplier tube. Some loss of light will inevitably take place due to some of the light traveling through 256 scintillator-epoxy interfaces. Further light loss takes place when the light travels down the optical fibers. The light then hits the photocathode surface of the photomultiplier tube. Since each scintillation must be detected by four photomultiplier tubes (to determine which ring, row, section, and column), each of the four photocathode surfaces must produce at least one photoelectron in order for the scintillation to be recorded. Both gamma rays from the positron-electron annihilation must produce a scintillation which in turn must be detected by four photomultiplier tubes in order for the position of the positron-electron interaction to be determined. Therefore, a total of eight photomultiplier tubes must produce a coincidence to detect each gamma ray pair. The purpose of this research is to find the probability that a scintillation will be detected.

CHAPTER II

GAMMA RAY – SCINTILLATOR INTERACTION

As the name "Positron Emission Tomograph" implies, the radiation from the subject's body comes from positron-emitting isotopes. The positrons interact with nearby electrons resulting in positron-electron annihilation. This results in two 0.511 MeV ($= m_o c^2$) gamma rays being emitted anti-parallel to each other within a range of about 0.6 degrees [1]. These two gamma rays then leave the body and interact with scintillators surrounding the patient.

Nearly all the interactions between plastic scintillators and gamma rays having an energy from about 0.1 MeV to about 5 MeV are due to Compton scattering [2]. The theoretical energy distribution of the recoil electrons resulting from Compton scattering by the 0.511 MeV gamma rays are shown in (Fig. 3). Since scintillation light output is nearly linearly proportional to the electron's kinetic energy [3], the relative shape of the Compton electron energy distribution should be the relative shape of the scintillation light pulse height distribution. This, of course, is assuming that the gamma ray was not scattered before entering the scintillator, thus lowering the energy of the gamma ray below 0.511 MeV. Furthermore, it is assumed that the recoil electron stays inside the scintillator. Recoil electrons from a 0.511 MeV gamma ray scattering event have a range within the plastic scintillator of about 0.9 mm when recoiling in the forward direction and up to about 0.3 mm in the transverse direction otherwise [4] (Fig. 4). Since the radial dimension of the scintillator is 10 mm and the width is 2 to 3 mm, only a small percentage of the electrons will escape the scintillator. If an electron does pass out of the scintillator, then less light will be produced, thus distorting the pulse height distribution.

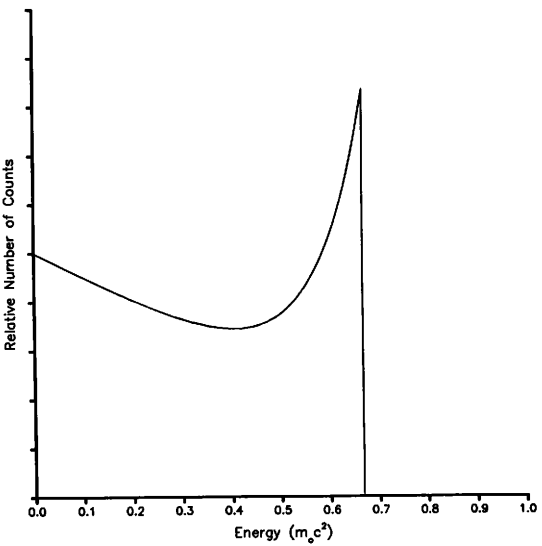

Fig. 3. Theoretical Compton Distribution

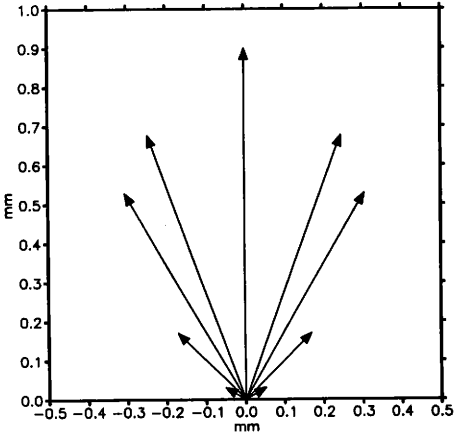

Fig. 4. Range of electrons in plastic scintillator.

CHAPTER III

LIGHT TRANSMISSION FROM THE SCINTILLATOR TO THE PHOTOMULTIPLIER TUBE

A. Light Transmission through the Scintillator

When a gamma ray interacts by Compton scattering inside the plastic scintillator, a flash of light is produced. For plastic scintillator NE102, a bluish light is produced which has a narrow wavelength spectrum that peaks at 423 nm. The pulse has a rise time of 0.9 ns, pulse width of 2.7 ns FWHM, and a decaying time constant of 2.4 ns [4]. This is much shorter than the more commonly used scintillators NaI(Tl) which has a decay constant of 230 ns [5] and BGO which has a decay constant of 300 ns [6]. The relative number of photons produced in NE102 is 28% of that produced by NaI(Tl) but 353% of that produced by BGO [7][6].

When a flash of light is produced, it must travel by means of internal reflection down a row and column within an array of scintillators. Light losses within the scintillator can come from light being absorbed by the scintillation material itself, by scattering off scratches on the surface of the scintillator, and by reflections produced when passing through a change in index of refraction.

NE102 is fairly transparent to its own light with an attenuation length of $a = 250$ cm [7], where the fractional absorption of light is $1 - e^{-x/a}$ and x is the length of the path the light travels through the scintillator. The largest path the the light could possibly travel is 76.8 cm. On the average, light will travel through only half that length to give an average absorbtion of 14%.

By using small polishing grit, the size of the scratches left by the polish was made smaller than the wavelength of the blue light, therefore producing an optically smooth surface. The reflections from the light passing through different indices of

refraction cannot be eliminated. The epoxy used to glue the scintillators together must have a lower index of refraction than the scintillator in order to achieve the total internal reflection necessary to allow the light to travel down the row and column of an array of scintillators. The index of refraction of NE102 is 1.581 [4] while that of the VA-6 epoxy [8] is 1.503. This 4.9% difference in indices of refraction allows a solid angle of $0.0247 \times 4\pi$ steradians to be transmitted by means of total internal reflection. Such a scintillator-epoxy interface produces a reflectance of 6.40×10^{-4} (transmittance of 0.999360) for light perpendicular to the interface. There are 255 such places along a row of scintillators where epoxy lies between two scintillators. Reflections occur at both the scintillator to epoxy and epoxy to scintillator interfaces, resulting in 510 reflections. Since a scintillation may take place anywhere along the row, light will, on the average, need to travel only half the length of the row through 255 interfaces to give an average of 85% of the light reaching the end of the scintillator row. When the light leaves the last scintillator's outer surface an additional 5% light loss from a scintillator-air interface will take place unless an optical grease is used instead of air to provide a better coupling between the scintillator and the adjoining optical fibers.

B. Light Transmission through the Optical Fibers

The light is transmitted from the array of plastic scintillators to the photomultiplier tube by means of optical fibers. Light losses from using optical fibers take place at the interface where the light enters the fibers, absorption of light by the fiber material, and at the other interface where the light exits the fiber.

Optical fibers transmit light down their length by means of total internal reflection. As a result, the incoming light must be within a certain angle in order to be transmitted down the entire length of fiber (Fig. 5). The fibers will accept light

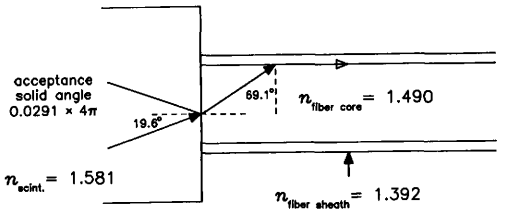

Fig. 5. Optical Fiber Acceptance Angle

from the scintillator within a solid angle of $0.0291 \times 4\pi$ steradians (as measured inside the scintillator). Since the solid angle of light that will be transmitted down the length of scintillators is $0.0247 \times 4\pi$ steradians, the light transmitted by total internal reflection in the scintillators should be transmitted down the optical fiber (except for reflections at the interface). At each end of the optical fiber, reflections may take place that add to the light losses. These losses will be about 7.6% (transmission = 92.4%) for perfectly polished fiber ends. This loss can be reduced by using an optical grease coupling on both ends of the fibers.

The light being transmitted down the fiber is also absorbed by the fiber material itself. The fraction of light being absorbed is $1 - e^{-\alpha x}$ where α is the absorption constant and x is the length of the fiber. The α for Crofon plastic optical fibers for light of wavelength $\lambda = 423$ nm is approximately 0.0113 cm^{-1} [9]. The TAMU PET calls for fiber lengths of 2 ft and 4 ft. The 2 ft fibers lose about 50% and the 4 ft fiber lose about 75%.

CHAPTER IV

THE PHOTOMULTIPLIER TUBE

A. The Photocathode Surface

Up until this point, the only possible source of efficiency reduction that has been mentioned is light loss. This has been done without describing how loss of light will affect the efficiency of the system. It is important to distinguish the difference between loss in the intensity of the light and loss in the number of light pulses. Ignoring quantum effects, even when light losses do take place the total number of light pulses remains constant (Fig. 6). If one could use an "ideal" photomultiplier tube that could detect an arbitrarily dim pulse of light, then these light losses would have no effect on the efficiency of the PET since the total number of pulses detected would not change. In reality however, loss in intensity results in a decrease in the total number of light pulses detected.

It is at the photomultiplier photocathode surface that the light losses are actually translated into reduction in efficiency of the PET. When light strikes the photocathode surface, electrons are emitted by means of photoemission [10]. A single photon of energy $h\nu$ greater than the work function ϕ of the material can cause a single electron, called a photoelectron, to be emitted. The quantum efficiency, **q**, is the probability that an incident photon will produce a photoelectron. For typical photocathode surfaces, **q** is about 20-30%. The particular photocathode surface used in this experiment was a bialkali surface which has an specified quantum efficiency of about 25% at a wavelength of 423 nm [11].

The number of photoelectrons that are produced is described by Poisson statistics. The probability that n photoelectrons will be produced is $P = \frac{<m>^n}{n!}e^{-<m>}$ where $< m >$ is the mean number of photoelectrons produced and is equal to

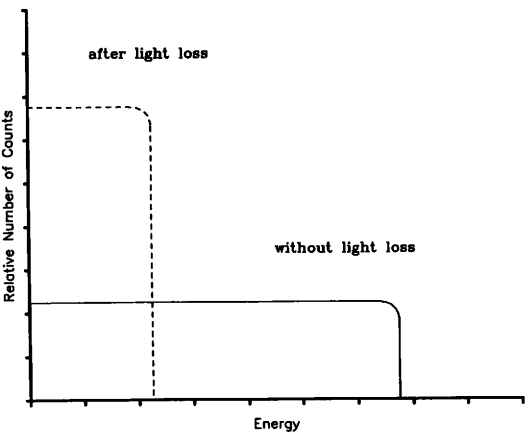

Fig. 6. Hypothetical pulse height distribution undergoing light loss.

$q < p >$. The term $< p >$ is the mean number of photons hitting the photocathode surface and is equal to $t < \Phi >$ where $< \Phi >$ is the mean number of photons being produced and t is the coefficient of transmission from the scintillator to the photomultiplier tube. The chance that no photoelectrons will be produced at all is $e^{-<m>}$. Production of an electron translates into detection of a scintillation. These detections are later coded into digital signals which indicate that a scintillation was detected. It does not matter how many photoelectrons are produced, but whether or not any are produced at all. Therefore, in order for the scintillation to be detected, at least one photoelectron must be produced. The probability that l photomultiplier tubes observing the same pulse of light will each produce at least one photoelectron is $\prod_l (1 - e^{-q_l < p_l >})$. For a given pulse height distribution $f(< \Phi >)$, the number of pulses detected by all l photomultiplier tubes would be $\int \prod_l (1 - e^{-q_l < p_l >}) f(< \Phi >) d\Phi$. Dividing this by the number of light pulses occurring gives the scintillation detection efficiency.

$$\frac{\int \prod_l (1 - e^{-q_l < p_l >}) f(< \Phi >) d\Phi}{\int f(< \Phi >) d\Phi}$$

In addition to photoelectrons, the photocathode also produces electrons by thermal emission. These electrons are refered to as the dark current of the photocathode as they are produced even in total absence of light. This dark current is heavily dependent on temperature. When thermal emission takes place, the electrons produced behave exactly like photoelectrons. Gamma rays directly striking the glass and photocathode surface knock off electrons which also behave like photoelectrons. The electrons produced by this effect are refered to as glass counts. Techniques for differentiating between photoelectrons, thermal emission electrons, and glass counts are discussed in chapters 5 and 6.

B. Amplification of Electrons

Once a photoelectron is produced, it is directed by an electrostatic field to a dynode. This field is set up by a high voltage between the photocathode and the first dynode. Upon striking the dynode, a number of secondary electrons are emitted and are accelerated toward a second dynode. Each electron striking the second dynode produces yet more electrons. This process continues for a total of typically 6 to 14 dynodes to provide a substantial current gain. A single electron emitted from the photocathode surface can produce a current pulse containing on the order of 10^6 electrons at the anode. The current collected at the anode is then carried outside the photomultiplier tube.

In addition to multiplying the number of electrons, the photomultiplier tube also produces dark current besides the thermal emission of the photocathode mentioned in the previous section. Dark current produced in the "multiplier" section of the tube is due to a number of regenerative effects [10]. These include electron bombardment of the dynodes which can produce a glow of light that can be reflected back to the photocathode, and also electrons being emitted from the first dynode without being induced by a photoelectron. Except at very high voltages, these effects are usually smaller than the noise produced by thermal emission from the photocathode.

The particular photomultiplier tube used was the Thorn EMI 9839B.

CHAPTER V

ELECTRONICS

A. Photomultiplier Tube Output

After the current is amplified inside the photomultiplier tube, it is collected by the the last dynode to obtain positive pulses and carried to electronic circuits used to interpret the signals. The photomultiplier tube is plugged into a base which provides the high voltage necessary for the amplification. The output of each photomultiplier tube is put through a voltage follower (LM310N) to provide current gain. The output of each voltage follower is then put into the main circuit board for detecting coincidences.

B. Coincidence Counting

The signals coming from the base are processed into logic pulses (Fig. 7). The signals are first put through a voltage comparator (LM361) to reject any pulses which are smaller than a particular voltage set by the bias level. This is used to eliminate pulses smaller than those produced by one photoelectron. The output of the comparator is a logical true when the input voltage is higher than the voltage being compared against (the bias voltage) and is a logical false otherwise. This output signal is then put into a monostable multivibrator (121, sometimes called a one-shot). When the multivibrator detects a positive input transition, it produces a high output for a specific period of time, independent of the duration of the input pulse. The output of the multivibrator then enters an AND gate, so that when all four multivibrators are "on" at the same time, the AND gate will produce a logic pulse. In the TAMU PET, these pulses will then enter one more AND gate to determine the actual coincidence that occurred with the detection of the other

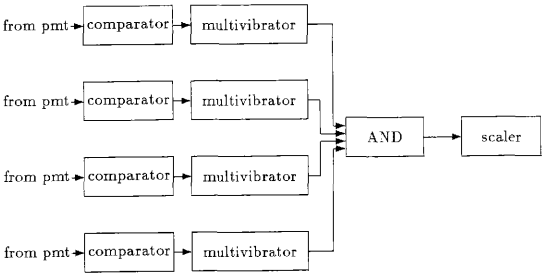

Fig. 7. Schematic of coincidence circuit.

gamma ray produced in the positron-electron annihilation. This additional gate, however, is not necessary for measuring the efficiency of the TAMU PET.

The comparators mentioned above are set so that pulses from the photomultiplier tube are rejected when they are smaller than about half the average size pulse produced by a single electron being emitted from the photocathode surface. This voltage value varies depending on the photomultiplier tube and the high voltage being used. The thermal emission electrons (chapter 4 section B), however, are amplified just as the photoemission electrons are and therefore the electric signals they produce will be larger than the comparator voltage. As a result, the photomultiplier tubes are continually giving false signals that are not rejected by the comparator. These false signals occur randomly in each tube. By making the multivibrator output pulses have durations of 100 ns, accidental coincidences between two tubes can be greatly reduced. When more than two photomultiplier tubes are used in coincidence, the accidentals can essentially be eliminated.

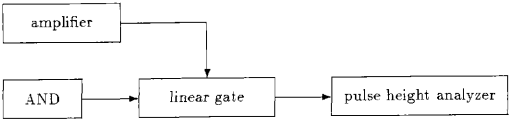

Fig. 8. Schematic of circuit for pulse height distribution.

C. Analyzing Pulse Height Distribution

In the TAMU PET, the size of the electrical pulses coming from the photomultiplier tube is not important as long as they are larger than the comparator voltage (section B). However, the pulse height distribution of the photomultiplier tube output is very important in understanding the efficiency of the PET and how it can be improved. To study this distribution, the output of the photomultiplier tube is put through an integrating amplifier and into a pulse height analyzer. A linear gate may be put between the amplifier and the analyzer to collect only the pulses that were larger than the comparator voltage or pulses that were in coincidence with other photomultiplier tube output pulses (Fig. 8). The linear gate takes an input from the amplifier and a gate input from the output of the AND gate (section B). The amplified pulse is passed on to the pulse height analyzer only if there was a pulse from the AND gate at the same time.

CHAPTER VI

EFFICIENCY MEASUREMENT

A. Overview of Procedure

The stated purpose of this research is to determine the optical efficiency of the TAMU PET, that is, to find the probability that a gamma ray interacting with the scintillators will be detected by the PET. The ability of the PET to detect gamma rays is proportional to the square (due to the fact that there are two gamma rays that must be detected for each positron-electron interaction) of the probability that a scintillation will be detected by the PET. The probability that a gamma ray will interact with the scintillators can be easily calculated given the geometry of the scintillator arrangement. The probability that a scintillation will be detected by the PET is much more difficult to calculate with certainty because of the many variables involved, hence the need to measure this probability experimentally.

The concepts involved in experimentally determining the probability that a scintillation will be detected are rather simple. Using a positron source, which therefore emits 0.511 MeV gamma rays from positron-electron annihilation, the scintillation rate is measured with the source located at a specified distance from the scintillator. This rate represents the total number of scintillations occuring and is a "reference" with which to compare counting rates measured later. Using a source-scintillator arrangement with the same geometry as before, the scintillation light is then directed down lengths of optical fiber bundles to four photomultiplier tubes. The coincidence counting rate between the four tubes is measured and represents the scintillations that were actually detected by the PET. The efficiency is the ratio between the scintillations detected and the scintillations occuring.

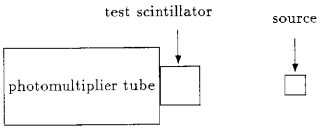

Fig. 9. Single photomultiplier arrangement.

In the TAMU PET, the only gamma rays used to produce a visual image are the 0.511 MeV gamma rays that have not been scattered prior to entering the scintillator in which the scintillation takes place. Therefore, when measuring these counting rates, it is important to count only the scintillations that were produced by previously unscattered 0.511 MeV gamma rays. Analysis of the scintillation light pulse height distribution is helpful in determining whether the detected scintillations were from unscattered gamma rays.

B. Determining the Number of Scintillations Occuring

Pulse Height Distribution with No Optical Fibers

Using plastic scintillator NE102 and a positron emitting 7.9 μCu ^{68}Ga source (decaying from ^{68}Ge, half life 275 days), a pulse height distribution was obtained. In addition to detecting scintillation pulses, the photomultiplier tube (Fig. 9) is also counting pulses from dark noise and glass counts (chapter 4). The effects due to the dark noise and glass counts were approximated by subtracting the pulse height distribution obtained with the photomultiplier tube covered with a sheet of black plastic. The black plastic blocked out the light from the scintillator while allowing the gamma rays from the source to pass through to the glass surface of the

photomultiplier tube. In order to collect as many pulses as possible, this reference measurement was made using a scintillator painted with titanium dioxide so that light emitted in all directions would be reflected into the photomultiplier tube, allowing more light to enter the tube. The paint also prevents distortion of the pulse height distribution. If the scintillator was not painted, then the photomultiplier tube would detect more light from a scintillation occurring near the tube face than it would had the scintillation occurred at the other end of the scintillator.

The resulting pulse height distribution (Fig. 10) was considerably different than the theoretical Compton distribution (Fig. 3). This indicates that the scintillator was detecting more than just the 0.511 MeV gamma rays. However, this measured pulse height distribution for the plastic scintillator is similar to measurements often reported in the scientific literature. The rounding off of the sharp Compton edge is expected due to the statistical nature of photon production in the scintillator, and photoelectron production and electron multiplication in the photomultiplier tube. The lower half of the distribution rises considerably higher than theory would indicate. Nardi suggests that this is due to gamma rays that have lost energy by scattering off of the walls, floors, etc., before interacting with the scintillator [2].

After doing an exhaustive literature search on the subject, no reported experiments could be found where the pulse height distribution for Compton scattering had been carefully measured down to the one photoelectron level. Because nearly all the interactions between 0.511 MeV gamma rays and plastic scintillators are due to Compton scattering, distinct energy level peaks are not produced as they are with NaI(Tl). As a result, plastic scintillators are generally used for applications where it is important to know the location of the Compton edge to determine the energy of incident monoenergetic gamma rays, or to know the relative height of the distribution to determine the overall magnitude of radiation incident on the

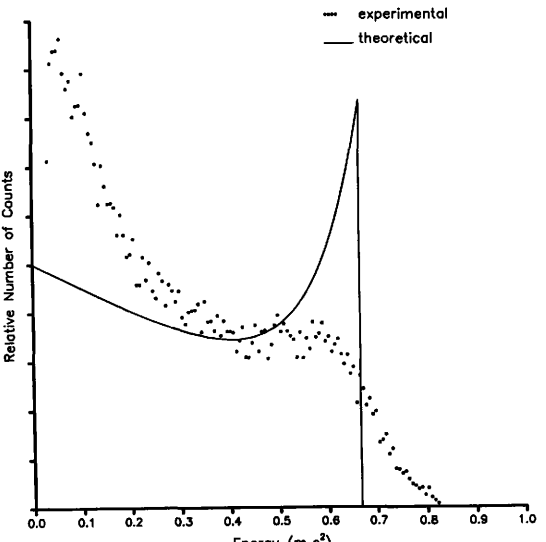

Fig. 10. Pulse height distribution from one photomultiplier tube.

detector. In both of these cases, the behavior of the pulse height distribution near the one photoelectron level is irrelevant and is therefore ignored.

In the TAMU PET, the pulse height distribution near the one photoelectron level greatly affects the overall efficiency and cannot be ignored. A constraint on the TAMU PET's design is the loss of light that takes place between the scintillator and the photomultiplier tube (chapter 3). As a result, in order to count as many light pulses as possible, the voltage comparators, which determine the threshold pulse size that will be recorded by the PET, are set to approximately one half the average voltage of a pulse produced by a single photoelectron being emitted from the photocathode surface. This allows weak pulses of light that only produced one photoelectron to be detected. The random dark noise pulses will be larger than the threshold voltage, but will be eliminated by the coincidence circuits (chapter 5 section B). The small scintillation light pulses that produce only one or two photoelectrons at each of the four photomultiplier tubes will not be eliminated by the coincidence circuit but will be counted just as if the pulse had produced 100 photoelectrons at each photomultiplier tube. Therefore, it is important to know how much of the pulse height distribution is in the one photoelectron region (Fig. 11).

In order to eliminate the scattered gamma rays in Fig. 10, a two-fold coincidence arrangement was used (Fig. 12). Since two gamma rays are emitted in nearly opposite directions from a positron-electron annihilation reaction, a scintillator coupled to a photomultiplier tube was placed on each side of the source. The chance that both gamma rays would be scattered and then both hit a scintillator is extremely small. Essentially, only the pulses produced by unscattered gamma rays would be in coincidence and therefore be counted. This coincidence is achieved at the cost of losing a fraction of the total number of counts. Since plastic scintillator

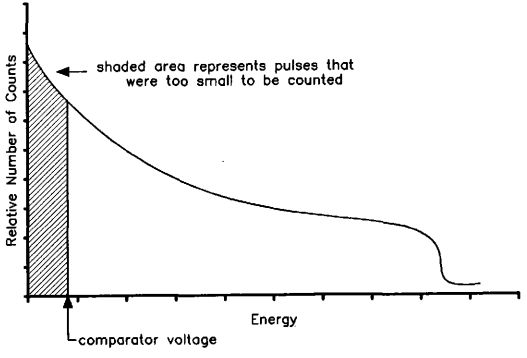

Fig. 11. Example of how low energy pulses affect efficiency.

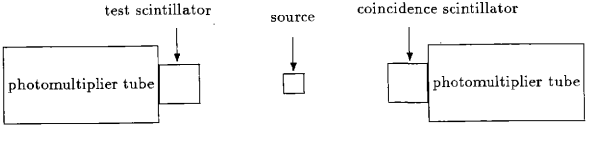

Fig. 12. Two-fold coincidence arrangement.

NE102 has an absorbtion coefficient of 0.0968 cm^{-1} for 0.511 Mev gamma rays, if an unscattered gamma ray had an interaction with the test scintillator, there was a 38% chance that the other gamma ray would interact with the 5 cm long coincidence scintillator. Although background subtractions still had to be made, the random dark noise was greatly reduced by the two-fold coincidence. The result of the measurement was a pulse height distribution that was much closer to the theoretical Compton distribution (Fig. 13). This means that, for the most part, the pulses that are counted using this arrangement are from unscattered 0.511 MeV gamma rays which used in to the TAMU PET.

Counting Scintillations with No Optical Fibers

Having shown that the effects of scattered gamma rays, dark noise, and glass counts can be eliminated, the measurement of the efficiency of the PET was then made. The same two scintillator two-fold coincidence arrangement mentioned earlier (Fig. 12) was used. This included the painted test scintillator coupled to a photomultiplier tube and the coincidence scintillator coupled to a photomultiplier tube on the opposite side of the source. A 25 mCu ^{64}Cu (half-life = 12.9 hr.) source (produced at the Nuclear Science Center) was used to increase the counting rates. The output of the two photomultiplier tubes was put through coincidence circuits and into a scaler (Fig. 7).

In order to make the most accurate counting measurements possible, further corrections were made. There is a chance that one photomultiplier tube will detect a scintillation while the other photomultiplier tube simultaniously detects a different scintillation. Accidental coincidence counts were reduced with 100 ns resolution in the coincidence circuits. The number of accidental counts was estimated using the

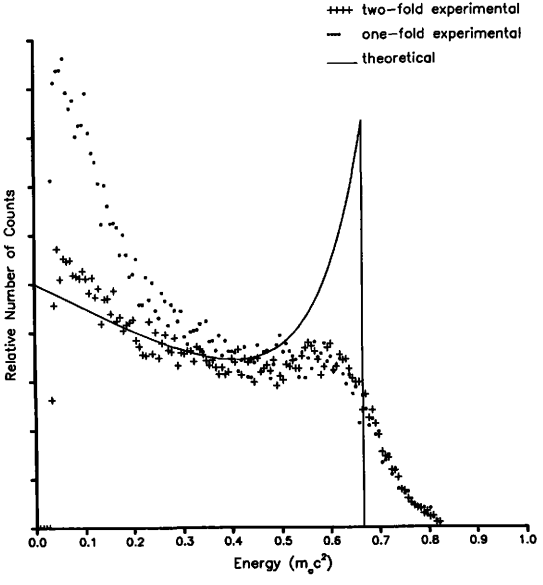

Fig. 13. Pulse height distribution for two-fold coincidence.

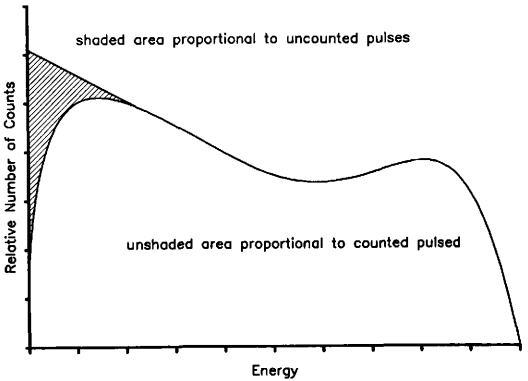

Fig. 14. Estimation of uncounted pulses.

following formula:

$$C = 2\tau N_1 N_2$$

where C = the accidental counting rate, τ = the time resolution, N_1 and N_2 = the counting rates involved.

Even though the test scintillator was painted and was against the photomultiplier tube face, there were still a few scintillation pulses that were too small to be detected by the photomultiplier tube. The number of undetected pulses were estimated by extrapolating the pulse height distribution curve back to the y-axis. The area between the extrapolated line and the measured distribution is proportional to the number of uncounted pulses (Fig. 14). The sum of the corrected measured pulse rate plus the estimated uncounted pulses gives the total of scintillations rate that occurred.

In the measurement with the painted scintillator, corrections were made for (a) glass counts on the photomultiplier tube that was coupled to the test scintillator, (b) accidental counts from two scintillations occurring at the same time, (c) uncounted scintillations, and (d) time of day to correct for the decaying isotope. Glass counts for the photomultiplier tube coupled to the coincidence scintillator were not subtracted. The 5 cm long piece of aluminum surrounding the coincidence scintillator stops 68% of the 0.511 MeV gamma rays so that nearly all the glass counts on that tube were from unscattered gamma rays that passed completely through the scintillator without being stopped. Since the purpose of the coincidence scintillator was to distinguish scattered from unscattered gamma rays, there is no need to subtract these unscattered gamma rays.

C. Determining the Number of Scintillations Detected

To measure the number of pulses that would be detected by the PET, a second scintillator was used which was identical in geometry to the painted one used in the previous section. These two scintillators had been glued together during the milling and polishing process to insure that both scintillators would have precisely the same geometry. This second scintillator was not painted, as was the previous one, but was coupled on all sides to lucite with the same epoxy glue used for the tomograph scintillator assembly. This was done to simulate the light being emitted out of all six surfaces of the scintillator rather than just one. The test scintillator was coupled via three 2 ft. and one 4 ft. optical fiber bundles to four photomultiplier tubes. These fiber lengths were selected to approximate the lengths used in the TAMU PET. The same coincidence scintillator used above was again coupled directly to a photomultiplier tube on the opposite side of the source. Hence, a five-fold coincidence circuit was used (Fig. 15) to measure the number of unscattered

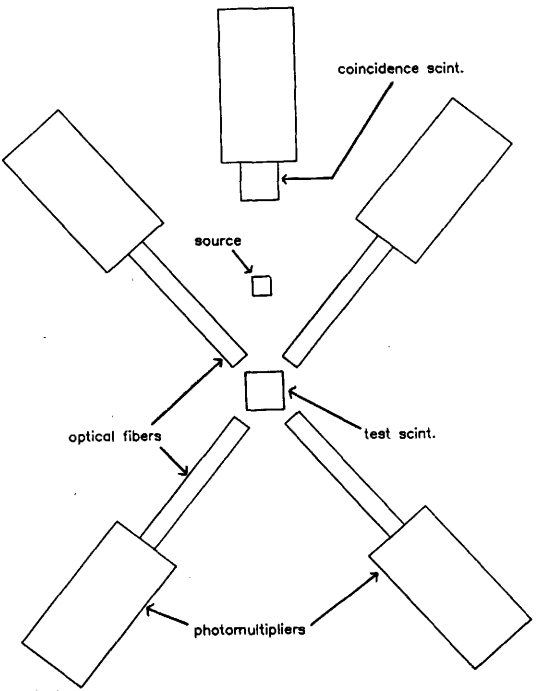

Fig. 15. Five-fold coincidence arrangement.

gamma rays that caused large enough light pulses to travel down the fiber bundles and still be detected by all four photomultiplier tubes. The fifth coincidence was the coincidence scintillator to assure that only unscattered gamma rays would be detected. Very few scattered gamma rays produce large enough pulses to be detected by the fiber-coupled photomultiplier tubes, even without this coincidence scintillator. However, this fifth coincidence is necessary if the coincidence pulse rate measured with the optical fibers in place is to be compared to the reference pulse rate using the painted scintillator. In the measurement with the optical fibers in place, the only corrections that needed to be made were the (a) accidental coincidences between two scintillations and (b) time of day to correct for the decaying isotope. The five fold coincidence eliminated all dark noise and glass counts.

D. The Efficiency

Once the corrected counting rates were determined, the probability of detecting a scintillation could then be found. This was simply the ratio between the scintillations detected with the five-fold coincidence and the scintillations occuring in the painted scintillator.

$$\text{detection efficiency} = \frac{\text{scintillations detected}}{\text{scintillations occuring}}$$

The random errors involved in making this measurement were small (on the order of 3%) due to the large number of counts involved. The main sources of uncertainty were due to systematic errors. Though the two-fold pulse height distribution (Fig. 13) was similar to the theoretical Compton distribution, there was still some disrepancy at the lower energies in the distribution. This amounted to about a 4% uncertainty in the number of pusles being counted. The extrapolation of the pulse height distribution to find the uncounted pulses was only an approximation (Fig.

14). However, since the estimated uncounted pulses amounted to only about 1% of the counted pulses, any uncertainties that result from this approximation are very small. The detection efficiency was found to be 0.29 ± 0.0145.

CHAPTER VII

FACTORS AFFECTING EFFICIENCY

Having measured the scintillation detection efficiency, it would be helpful to know how it could be improved. One important factor is the effect of the optical fibers on the light pulses. A pulse height distribution was obtained for the light coming out of one of the 2 ft. optical fiber bundles. The same scintillator with the lucite ports was used for the optical fiber test so that the light being collected would be, as in the tomograph, from only one sixth of the scintillator surfaces from which light can be emitted. The same source-scintillator geometry as before was used.

At this point, only the shape of the pulse height distribution was of interest. In order to keep the counting rate high with the weak ^{68}Ge source, the two scintillator coincidence arrangement was not initially used for measuring the pulse height distribution through the fibers. It was used for the efficiency measurement to eliminate the lower energy pulses that resulted from the scattered gamma rays and to reduce random noise from the photomultiplier tube, thereby providing a reliable reference pulse height distribution. With the fibers, much of the light was lost and the smaller pulses from the scattered gamma rays were too small to be detected by the photomultiplier tube. The problem of glass counts and random noise was eliminated by placing three other photomultiplier tubes at the ends of the lucite ports coming out of the scintillator (Fig. 16). Any pulse of light that could go through the optical fibers and be detected by the photomultiplier tube on the other end of the fibers could be assumed to be detected by the photomultiplier tubes adjacent to a lucite port. Thus, there was a four-fold coincidence using three photomultiplier tubes all coupled to a single scintillator and a fourth photomultiplier tube connected by optical fibers to the same scintillator. This arrangement eliminates the random

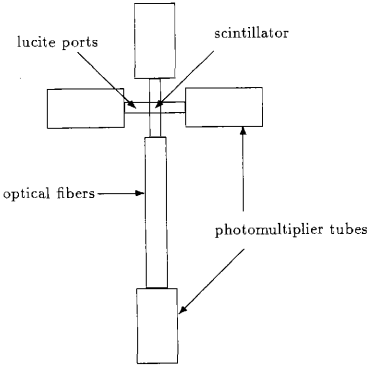

Fig. 16. Four-fold coincidence arrangement for optical fiber test.

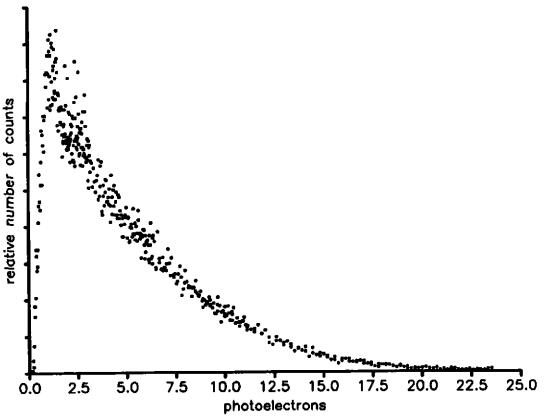

Fig. 17. Pulse height distribution of light from optical fibers.

noise while keeping the counting rate high. The same coincidence circuits were used as before.

The measured pulse height distribution of the light coming out of the other end of the optical fibers (Fig. 17) was drastically different than the pulse height distribution of the light going in (Fig. 13). The result no longer resembled a Compton distribution but decayed nearly exponentially. This is particularly undesirable considering that the larger the percentage of the pulses that are in the lower end of the distribution, the more the efficiency is reduced for a given amount of light loss (Fig. 11). On the other hand, small gains in the transmission of light from the

scintillator to the photomultiplier tube will mean large gains in the efficiency.

This measurement was repeated using a stronger 25 mCu ^{64}Cu source in the two scintillator two-fold coincidence arrangement with a scintillator on opposite sides of the source (Sect B). The coincidence scintillator was coupled directly to a photomultiplier tube while optical fibers joined the other scintillator with its photomultiplier tube. The measurement yielded a pulse height distribution similar to that of the one scintillator four-fold coincidence arrangement, thereby confirming that the small light pulses from scattered gamma rays are too small to be detected after transmission through the optical fibers.

These measurements have not only determined the scintillation detection effeciency but have also clarified the detection process. Thus, it is now more apparent how the efficiency can be improved. Though a number of aspects of the TAMU PET that cause light losses cannot be eliminated such as from reflections in the scintillator, there are a number of ways that efficiency can be increased . Two important sources of light losses that can be changed are the optical fibers and the photocathode surface. The four foot optical fibers attenuate the light by a factor of four (chapter 3 section B). New fibers from Eska (Mitsubishi) with a specified attenuation of only 1.07 per meter [12] are being prepared for testing. This would allow 3.6 times more light to pass through the 4 ft. fibers than the Crofon optical fibers. At the photocathode surface, any improvement in the quantum efficiency (chapter 4) directly increases the detection ability of the TAMU PET. Photomultiplier tubes with a 20% better quantum efficiency can be obtained. And finally, the use of optical couplings between the scintillators and the fibers and between the fibers and the photomultiplier tubes (not used in the measurements) will prevent a 20% loss in light transmission.

Combining these factors of $3.6 \times 1.20/(1 - .20) = 5.4$, the effect will be to push the pulse height distribution of light coming out of the optical fibers (Fig. 17) to the right by a factor of 5.4. This would increase the area above the threshold voltage and therefore would allow more of the pulses to be counted.

CHAPTER VIII

CONCLUSIONS

In conclusion, the goals of this research have been obtained. The scintillation detection efficiency was measured and found to be 0.29 ± 0.0145. The uncertainty was due mostly to systematic errors. Also, methods of improvements have been examined. Reduction in light losses by a factor of five can be feasibly acheived.

REFERENCES

[1] Muehllehner, G., "Resolution Limit of Positron Cameras," *J. of Nucl. Med.*, vol. 17, pp. 757, 1976.

[2] Nardi, E., "Gamma Ray Measurements with Plastic Scintillators," *Nucl. Inst. and Meth.*, vol. 95, pp. 229-232, 1971.

[3] Smith, D.L., Polk, R.G., Miller, T.G., "Measurement of the Response of Several Organic Scintillators to Electrons, Protons, and Deuterons," *Nucl. Inst. and Meth.*, vol. 64, pp. 157-166, 1968.

[4] "Premium Plastic and Liquid Scintillators – BC-400," Bicron Corp., Newbury, Ohio, n.d.

[5] Derenzo, S.E., "Positron Ring Cameras for Emission-Computed Tomography," *IEEE Trans. on Nucl. Sci.*, vol. NS-24 No.2, pp. 881-885, April 1977.

[6] Nester, O.H., Huang C.Y., "Bismuth Germanate: A High-Z Gamma-Ray and Charged Particle Detector," *IEEE Trans. Nucl. Sci.*, vol. NS-22, pp. 68-71, 1975.

[7] "Scintillators for the Physical Sciences," Nuclear Enterprise Ltd., Reading, England, pp. 3,9-11, n.d..

[8] "Preliminary Data on Experimental/Custom Formulated Product VA-6," Epoxy Technology, Inc., Billerica, Mass., 1977, updated 1983.

[9] Brown, R. G., Derick, B. N., "Plastic Fiber Optics. II: Loss Measurements and Loss Mechanisms," *Applied Optics*, vol. 7, No. 8, pp. 1565-1569, 1968.

[10] "Photomultiplier Handbook," RCA, Solid State Division, Electro Optics and Devices, Lancaster, Penn., pp. 11,12,56, 1980.

[11] "Photomultipliers," Thorn EMI Electron Tubes Ltd., Plainview, N.Y., pp. 20,21, 1982.

[12] "High-Performance Plastic Optical Fibers," Mitsubishi Rayon Co. Ltd., Eska Optical Fibers Division, Tokyo, Japan, p. 5, n.d.

VITA

Wesley Blake Loewer

BIRTH:

October 16, 1963, Eunice, Louisiana

FAMILY:

Married, Jane Shirk, August 22, 1987

EDUCATION:

Wheaton College (1981-85) B.S. in Physics.

Wesley B. Loewer

4302 College Main #129

Bryan, TX 77801